Kuwait Journal of Science 53 (2026) 100562

Contents lists available at ScienceDirect

Kuwait Journal of Science

journal homepage: www.sciencedirect.com/journal/kuwait-journal-of-science

Full length article

An equitable and safer multi-objective cycling network design approach to connect green and blue spaces ☆

Bruno Salezze Vieira [a,c,*], Ranga Abeysooriya [b], Dawn-Marie Walker [c], Edilson F. Arruda [a,d]

[a] University of Southampton Business School, Southampton, United Kingdom
[b] Faculty of Engineering, University of Moratuwa, Moratuwa, Sri Lanka
[c] University of Southampton, School of Health Sciences, Southampton, United Kingdom
[d] Centre for Healthcare Analytics, University of Southampton, Southampton, United Kingdom

ARTICLE INFO

Keywords:
Cycling network expansion
Location problem
Multi-objective optimisation
Exact methods
Heuristics

ABSTRACT

In urban planning, integrating green and blue (waterside) spaces via functional cycling networks is crucial for accessible and sustainable development, with clear links to healthier lifestyles and environmental benefits. This paper presents a multi-objective approach to cycling network expansion that optimises connectivity between green and blue spaces while accounting for cost, coverage, equitable access, and safety. The approach provides useful decision support with a set of non-dominated solutions, where all solutions generate fully connected paths between existing cycle infrastructure and green and blue areas. This guarantees that the network design is functional, cycle-friendly, safer, and conducive to active transportation. To validate the approach, we generate a menu of solutions for the city of Southampton, UK. The results illustrate the model's effectiveness in generating a network expansion design that connects existing cycling infrastructure to green and blue areas under different compromises among the criteria.

1. Introduction

Integrating green and blue (waterside) spaces within urban landscapes is essential for advancing sustainable development, improving environmental quality, and promoting active transportation. Well-designed cycling networks that connect these natural spaces are foundational to sustainable mobility, offering a clear pathway to reducing reliance on motorised transport and fostering urban livability (Davis, 2010; Gössling et al., 2024). Functional cycling infrastructure yields significant environmental, social, and public health benefits. It promotes active transportation, which helps reduce the prevalence of sedentary lifestyle-related health issues, mitigates health disparities, and improves accessibility in underserved communities (Le Gouais et al., 2021; Cunha and Silva, 2023). From an environmental perspective, cycling networks help alleviate congestion and lower transport-related emissions, improving urban sustainability (Kilani and Bennaya, 2023; Zahabi et al., 2016).

The effectiveness of cycling infrastructure expansion is also influenced by factors such as network continuity, accessibility, and integration with other modes of transportation. Research highlights the importance of addressing discontinuities in cycling networks to ensure a seamless and comfortable riding experience, as interruptions in bike lanes can reduce perceived safety and deter potential cyclists (Krizek and Roland, 2005). Additionally, the presence of dedicated cycling infrastructure has been found to increase cycling uptake, with new facilities encouraging greater bicycle commuting and reducing car dependency, particularly in urban areas (Mitra et al., 2021). Furthermore, integrating cycling infrastructure with public transit systems can enhance urban mobility, particularly in large, rapidly expanding cities, where bicycle-transit integration is crucial to sustainable transportation strategies (Zhao and Li, 2017).

It is crucial, however, to contextualise the challenge of network fragmentation. While research highlights the negative impacts of discontinuities, a practitioner's perspective reveals that these are often not the result of isolated design failures but rather the optimal outcomes of distributed, often unconnected policymaking layers that impose complex real-world constraints. Transport planners must frequently navigate competing demands for limited road space, inconsistent funding, and complex political landscapes (Aldred et al., 2019; Tiznado-Aitken et al.,

☆ This article is part of a Special issue entitled: 'OR trends & applications' published in Kuwait Journal of Science.

* Corresponding author at: University of Southampton Business School, Southampton, United Kingdom.
E-mail addresses: b.salezze-vieira@soton.ac.uk (B.S. Vieira), rangaa@uom.lk (R. Abeysooriya), dawn-marie.walker@soton.ac.uk (D.-M. Walker), e.f.arruda@southampton.ac.uk (E.F. Arruda).

https://doi.org/10.1016/j.kjs.2026.100562
Received 14 July 2025; Received in revised form 3 March 2026; Accepted 5 March 2026
Available online 10 March 2026

2022). Therefore, the central problem is not merely correcting design errors but making strategic, evidence-based decisions that explicitly balance competing objectives.

To address this reality, this paper proposes a decision-support tool designed to help planners navigate these inherent trade-offs. We introduce a multi-objective modelling approach to facilitate the strategic expansion of cycling networks while ensuring connectivity between green and blue spaces. This approach balances cost efficiency and network connectivity with environmental and social priorities by optimising the expansion of cycle infrastructure to enhance accessibility in socio-economically disadvantaged areas, while prioritising quieter, safer routes.

We explicitly prioritised a multi-objective modelling approach over traditional single-objective or weighted-sum methods. Whereas weighted-sum approaches obscure the true trade-offs by collapsing conflicting goals into a single scalar value, our approach empowers decision-makers with a menu of solutions that also displays all of their trade-offs. It uncovers cost increases associated with gains in equity and safety that would otherwise remain invisible in standard single-objective or weighted-sum approaches. The resulting framework provides planners with a structured methodology for evaluating trade-offs among competing objectives (Deb and Deb, 2014), offering a menu of planning alternatives aligned with sustainable urban development goals.

To tackle continuity and interconnection, the approach first maps fully connected cycle sub-networks (called cycle zones) and green and blue spaces (called green (blue) spaces) within the urban environment. We assume that each individual zone is fully connected and that people can move freely via active transportation within each zone. The model's output recommends additional cycle lanes to complement existing infrastructure and enhance connectivity under the proposed multi-criteria framework. To illustrate the approach, Fig. 1 shows a densely populated, deprived urban environment from the city of Southampton, UK. The marked green zones are the green spaces; the existing cycling infrastructure is highlighted in brown; the white and grey segments are the existing roads; and the blue segments are the suggested additional cycle lanes. The example comprises five purely cycling zones (B, C, D, E, and G), one purely green space (A), and two green spaces connected to cycling zones (F and H). The suggested additional cycle lanes directly connect zones A to B, B to C, C to F and F to H. It is perhaps noteworthy that the existing infrastructure in Fig. 1 exemplifies the connectivity issues that often discourage cycling among potential new users and raise additional safety concerns, as it forces cyclists into busy, non-cyclist-friendly car lanes.

The remainder of this paper is organised as follows. Section 2 reviews the related literature and summarises the positioning of our work. Section 3 introduces the proposed mathematical formulation. Section 4 explains the solution procedures and introduces the corresponding algorithms. To validate the approach, Section 5 presents a real-world example: the cycle network of the city of Southampton, in the south of England. It also presents an analysis of the set of non-dominated solutions for the decision-maker, highlighting potential trade-offs among objectives and their corresponding performance. The results illustrate the potential to provide local authorities with pertinent, actionable plans for effective cycle expansion that account for coverage, cost, quietness, and equity. Finally, Section 6 concludes the paper.

2. Literature review

Despite the recent trend towards green transportation, the development of the cycling infrastructure faces prohibitive barriers such as inconsistent funding, poor design and connectivity, and a lack of expertise, tools and models to support the planning of a new infrastructure (Aldred et al., 2019). Thoughtful planning of bicycle infrastructure is relatively recent, driven by the contemporary push towards sustainability, healthier lifestyles, and the integration of green and blue spaces into our daily lives (Dales et al., 2014).

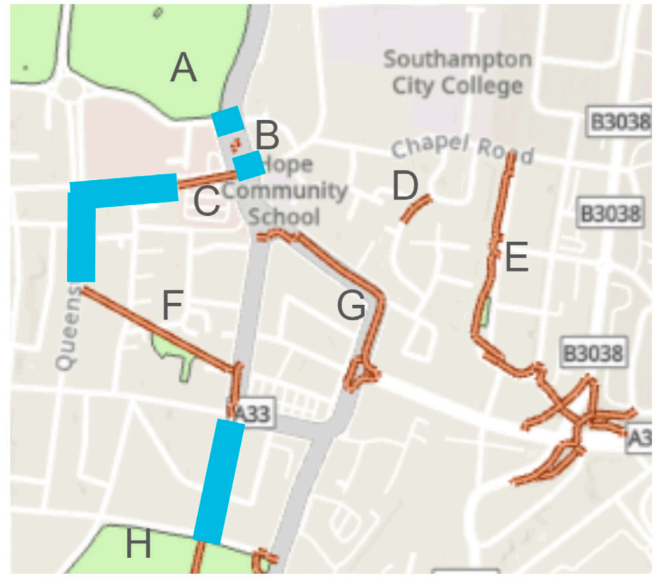

Fig. 1. Network example.

Mathematical programming is a natural approach to bicycle network design, employed across the literature, with diverse objectives and constraints that are mostly related to regional circumstances. In a case study in Austin, the approach proposed by Duthie and Unnikrishnan (2014) retrofits existing bicycle roadway infrastructure to connect multiple origin–destination pairs under budget constraints, whilst enforcing prescribed service levels. The rationale for using a system's approach rather than focusing on separate origin–destination pairs is also present to some degree in the formulation of Mauttone et al. (2017)'s framework, which considers user costs and network discontinuities in a case study in Montevideo. In contrast, Liu et al. (2019) embeds a logit model to capture route choice behaviour. They include the resulting equilibrium constraints in their cycle network design problem: a mixed-integer nonlinear nonconvex model solved using exact and metaheuristic methods. These studies underscore the importance of balancing objectives such as cost, accessibility, coverage, and connectivity in designing effective and sustainable bicycle networks. These principles closely align with the innovative multi-objective approach proposed in this paper.

The concept of balancing different aspects takes precedence in the study by de Oliveira et al. (2021), which introduces 14 objectives while considering constraints related to comfort, safety, connectivity, bus service connectivity, and budget. Their multi-objective mixed-integer linear programming (MILP) model is applied to a case study in Brazil, illustrating the multiple trade-offs at the planning phase. Their approach requires the decision maker to elicit trade-offs a priori by assigning weights to each objective, thereby transforming the multi-objective problem into an equivalent single-objective model. A related but less intricate multi-objective MILP model developed for Singapore focuses on retrofitting existing cycling infrastructure to maximise accessibility whilst also minimising costs and the total number of intersections (Zhu and Zhu, 2020). They utilise an ϵ-constraint and weighted-sum method to identify the set of non-dominated solutions (the Pareto front) and report scenarios that focus on a single objective at a time.

An approach centred on a case study in Medellin introduced a MILP model to maximise the connectivity of the cycling network subject to budget constraints (Ospina et al., 2022). This study emphasises the importance of creating safe and direct routes while allowing flexibility in travel paths. Under a different paradigm, Caicedo et al. (2023) utilised mathematical programming to support the design of shared bike networks, specifying parameters such as the length of cycle paths and the fleet size of a bike share service. The validation example in Guayaquil highlights the long-term viability of bike networks and suggests that increased demand does not necessarily require proportional investment. Finally, a study applied in Copenhagen undertakes a cost–benefit analysis of the long-term expansion of a cycle network (Paulsen and Rich, 2023). They introduce a reverse-geographical-mapping approach to allocate monetary benefits within the network, facilitating detailed geographical planning. These are then entered into a MILP model that evaluates the network design's benefit in terms of travel time savings. The output is a development plan that considers long-term benefits and highlights the importance of strategic prioritisation in bicycle network investments.

Qualitative and data-driven studies also provide useful findings and insights. For example, upon finding that cycle networks often consist of disconnected patches even in cycling-friendly cities, Natera Orozco et al. (2020) proposed ad hoc data-driven strategies to identify critical links for network augmentation, thereby improving connectivity and travel times. Their results suggest that small, focused investments can significantly enhance urban bicycle networks. A related study utilised multi-criteria decision analysis to prioritise corridors for cycle-path investment, considering costs, connectivity, network coverage, and automotive traffic delays (Zuo and Wei, 2019). A case study in Cincinnati demonstrates that protected bike lanes provide significant benefits for cyclists and transit users, potentially offsetting higher construction costs and potential traffic congestion. Another alternative is to combine multi-criteria decision analysis with geographic information systems (GIS) to prioritise potential locations for bike-sharing stations and lanes (Guler and Yomralioglu, 2021).

Also relevant to our study are papers concerning cyclists' behaviours and preferences. A case study in Ontario suggests that cyclists tend not to deviate much from the shortest path to their destination, whilst also keen to avoid high-activity areas (Aultman-Hall et al., 1997). Concurrently, a similar analysis in Vancouver found that cyclists detoured to routes with better bicycle facilities, such as traffic-calming features and dedicated bike paths, even if they were longer (Winters et al., 2010). These findings highlight that multiple factors beyond travel time influence cycling behaviour, including the cycling infrastructure's quality and functionality and the cycling paths' perceived safety. Connection to green spaces is also meaningful, as highlighted in a study of GPS and GIS data on the routes taken by cyclists in Graz, Austria (Krenn et al., 2014). Unsurprisingly, the study found that cyclists avoided main roads and crossings and preferred dedicated bicycle lanes and flat green areas. For a comprehensive review of the multiple factors in the strategic and operational planning of bike-sharing systems, refer to Nath and Rambha (2019).

Thus, the uptake of cycling infrastructure may relate to users' perceptions and to its connections with other modes of transport, such as trains. For example, a study in the Netherlands found that attitudes towards cycling and the frequency of train use are essential factors in cycling uptake (Paix et al., 2021). More generally, a study of cycle infrastructure across 62 cities found that network development initially exhibits decreasing returns on investment until a critical threshold is reached, suggesting that persistent, strategic investment is necessary to achieve a critical mass for effective bicycle networks (Szell et al., 2022). This is somewhat intuitive, as other studies found that cycling infrastructure tends to be disconnected (e.g., Natera Orozco et al., 2020). Hence, several iterations of new infrastructure may be required until the cycling network reaches connectivity and functionality levels acceptable to the average cyclist. A related study in Bogotá conducted a survey that found six factors associated with cyclists' perceived quality of service, comprising safety and environmental factors (Barrero and Rodriguez-Valencia, 2022). The findings challenge traditional supply-oriented evaluation methods and advocate for incorporating user perceptions into the design and evaluation of bicycle infrastructure, highlighting the need for cyclist-centred planning.

Table 1 synthesises the key characteristics of relevant studies discussed in this section, positioning our proposed approach within the broader literature. The columns detail the *methodology* employed (e.g., MILP, heuristics, or data-driven analysis) and the *key objectives* prioritised in each study. Crucially, the comparison distinguishes studies based on their optimisation framework: the *multi-obj* column indicates whether multiple conflicting goals are explicitly considered. In contrast, *exact Pareto* specifies whether the method generates a proper set of non-dominated solutions (Pareto front). Finally, the columns *green/blue* and *equity* highlight the specific inclusion of environmental space connectivity and social deprivation metrics.

Scientific contributions. This work proposes a multi-objective approach to cycle network design with three unique contributions to the literature:

1. **Green and blue space connectivity:** In line with the contemporary push towards vibrant urban communities (e.g., Davis, 2010; Tiznado-Aitken et al., 2022), and considering that cyclists value contact with nature (Krenn et al., 2014), we propose an innovative approach that explicitly enforces fully connected paths between existing cycle infrastructures and green and blue areas.
2. **Equity and quietness as primary objectives:** We pioneer the inclusion of equity (based on deprivation indices) and quietness (as a proxy for safety) as primary optimisation objectives rather than secondary constraints. This addresses the critical need for inclusive networks that do not exclude future generations or underserved communities due to safety concerns (Cunha and Silva, 2023; Gössling et al., 2024).
3. **Exact Pareto optimisation:** In line with Zhu and Zhu (2020), we avoid the common practice of establishing arbitrary weights to transform a multi-objective problem into a mono-objective one. Instead, we solve the problem utilising exact methods to derive a set of non-dominated solutions, the *Pareto front*. This provides decision-makers with a transparent "menu" of designs, quantifying exactly how much connectivity must be traded off to achieve specific gains in equity or safety.

The next section will formalise our problem using a multi-objective mathematical model that aims to minimise cost, maximise connectivity, maximise quietness, and maximise equity. These are often conflicting objectives, which are later solved in Section 4 and will yield a set of non-dominated solutions (Pareto front).

3. Mathematical model

Consider an urban environment described by a road network $G = (N, E)$ comprised of a set of nodes N and a set of directed edges E. Each edge represents a road segment, and each node represents an intersection. We further split the set of nodes N into two disjoint subsets: subset $P \subset N$ contains all nodes within a cycle, green or blue zone; subset $I = N \setminus P$ contains all the remaining nodes. Furthermore, let $Z \vdash P$ be the set of zones, a partition of P. Each zone $a \in Z$ represents all the nodes within a specific green, blue, or cycle zone. For each road segment $(i, j) \in E : i, j \in N$, $c_{ij} > 0$ is the cost to link nodes i and j via a cycle-way, $q_{ij} > 0$ is the quietness contribution of this link to the overall solution and $e_{ij} > 0$ is the link's equity contribution. The numerical values of each contribution are detailed and discussed after our experimental description in Section 5 with our data sources.

For each edge $(i, j) \in I$ not belonging to a cycle, green or blue zone, the binary decision variable $x_{ij} = 1$ if this edge is selected for cycling expansion; otherwise $x_{ij} = 0$. Another binary variable y_{ab} will be created for each pair of zones $a, b \in Z, a \neq b$ to map connectivity: $y_{ab} = 1$ if zones a and b are directly connected, which means that there exists at least a cycling route linking this pair of zones without passing through any other zone in Z, and $y_{ab} = 0$ otherwise. Binary variable

Table 1
Summary of related literature and contributions.

Reference	Methodology	Key objectives/Focus	Multi-Obj	Pareto		Green/Blue	Equity
				Exact	Aproxim.		
Duthie and Unnikrishnan (2014)	MILP	Retrofitting, Cost, Level of service	–	–	–	–	–
Mauttone et al. (2017)	MILP	User cost, Discontinuities	–	–	–	–	–
Liu et al. (2019)	MIP (-n-convex)	Route choice, Equilibrium constraints	–	–	–	–	–
de Oliveira et al. (2021)	MILP	14 objectives (Weighted Sum)	✓	–	–	–	–
Zhu and Zhu (2020)	MILP (Heuristic)	Accessibility, Cost, Safety	✓	–	✓	–	–
Ospina et al. (2022)	MILP	Max connectivity, Budget	–	–	–	–	–
Paulsen and Rich (2023)	CBA + MILP	Cost-benefit analysis, Travel time	–	–	–	–	–
Natera Orozco et al. (2020)	Data-Driven	Connectivity, Critical links	–	N/A	N/A	–	–
Zuo and Wei (2019)	MCDA	Investment prioritisation	✓	N/A	N/A	–	–
This paper	**MIP (Solver)**	**Conn., Cost, Quietness, Equity**	✓	✓	–	✓	✓

$f_a = 1, a \in Z$ if there is at least a cycle route from a to a different zone $b \in Z$ and $f_a = 0$ otherwise. Analogously, $b_a = 1$ if there exists a cycle route that can reach a starting from a different zone $b \in Z$, and $b_a = 0$ otherwise.

The variables ϕ_{ija} are flow variables used to ensure connectivity between the zones if some variable y_{ab}, b_a, or f_a is active. For each edge $(i,j) \in E$ and zone $a \in Z$, $\phi_{ija} = 1$ if there is at least a cycle route from zone a that reaches node j immediately after reaching node i, and $\phi_{ija} = 0$ otherwise. Finally, for any set of nodes $a \subset N$, let $\delta^-(a) := \{(i,j) | (i,j) \in E, i \in a, j \notin a\}$ be the set of edges leaving a and, analogously, $\delta^+(a) := \{(i,j) | (i,j) \in E, i \notin a, j \in a\}$ be the set of edges entering a.

To facilitate the reading, Table 2 summarises the notation and describes the sets, attributes, parameters, and model variables. The full mathematical formulation of our multi-objective problem is as follows - Eqs. (1)–(16).

$$\text{Maximise} \sum_{a \in Z} f_a + b_a \tag{1}$$

$$\text{Minimise} \sum_{(i,j) \in E} c_{ij} x_{ij} \tag{2}$$

$$\text{Maximise} \sum_{(i,j) \in E} q_{ij} x_{ij} \tag{3}$$

$$\text{Maximise} \sum_{(i,j) \in E} e_{ij} x_{ij} \tag{4}$$

Subject to:

$$x_{ij} \geq \phi_{ija} \ \forall (i,j) \in E, \forall a \in Z \tag{5}$$

$$\sum_{a \in Z} \sum_{(i,j) \in \delta^+(b)} \phi_{ija} \geq b_b \ \forall b \in Z \tag{6}$$

$$\sum_{(i,j) \in \delta^+(a)} \phi_{ija} = 0 \ \forall a \in Z \tag{7}$$

$$\sum_{(i,j) \in \delta^-(a)} \phi_{ija} \geq f_a \ \forall a \in Z \tag{8}$$

$$\sum_{a \in Z, a \neq b} \sum_{(i,j) \in \delta^-(b)} \phi_{ija} = 0 \ \forall b \in Z \tag{9}$$

$$\sum_{a \in Z} \sum_{(i,j) \in \delta^-(\{n\})} \phi_{ija} = \sum_{a \in Z} \sum_{(i,j) \in \delta^+(\{n\})} \phi_{ija} \ \forall n \in I \tag{10}$$

$$\sum_{(i,j) \in \delta^-(b)} \phi_{ija} \geq y_{ab} \ \forall a, b \in Z, a \neq b \tag{11}$$

$$\sum_{a,b \in S, a \neq z} y_{ab} \leq |S| - 1 \ \forall S \subset Z \tag{12}$$

$$x_{ij} \in \{0,1\} \ \forall (i,j) \in E \tag{13}$$

$$f_a, b_a \in \{0,1\} \ \forall a \in Z \tag{14}$$

$$\phi_{ija} \in \{0,1\} \ \forall (i,j) \in E, \ \forall a \in Z. \tag{15}$$

$$y_{ab} \in \{0,1\} \ \forall a, b \in Z, a \neq b. \tag{16}$$

The first objective (1) is to maximise connectivity, measured as the total number of connections between zones. The second objective (2) is to minimise the total network expansion cost. The third objective (3) is to maximise the overall *quietness* of the network, as a proxy for safety. Finally, the last objective (4) is to maximise equitable contributions.

Constraints (5)–(10) control the flow on the network and how they regulate variables x, f, and b. Essentially, zones source their own flow and sink flow from other zones while intersection nodes conserve flow. More specifically, the set of constraints in (5) ensures that the road segment is selected if any flow traverses it. Constraints (6) ensure that a zone is reached if any flow enters it, and (7) ensures that any flow that enters a zone must come from a different zone. The set of constraints in (8) ensures that a zone reaches another if any flow leaves it, and (9) ensures that flows from other zones are sunk. Constraints (10) ensure flow conservation for each intersection node. Constraints (11) ensure a connection from zone a to zone b if flow coming from a is sunk on b. Constraints (12) prevent cycles between zone connections. Finally, constraints (13)–(16) define the variables' domains.

To help derive the Pareto front via single-objective sub-problems, we introduce constraints (17)–(20) that bound the solutions to each respective objective (objectives (1)–(4)). This will be further clarified in Section 4. In the following inequalities, parameters $\alpha > 0$, $\beta > 0$, $\delta > 0$, and $\gamma > 0$, respectively, represent the target objective value in the formulation:

$$\sum_{a \in Z} f_a + b_a \geq 2\alpha, \tag{17}$$

$$\sum_{(i,j) \in E} c_{ij} x_{ij} \leq \beta, \tag{18}$$

$$\sum_{(i,j) \in E} q_{ij} x_{ij} \geq \delta, \tag{19}$$

$$\sum_{(i,j) \in E} e_{ij} x_{ij} \geq \gamma. \tag{20}$$

The solution strategy for the formulation in Eqs. (1)–(20) will be detailed in Section 4 and subsections therein. Essentially, we will solve a bi-objective formulation considering objectives (1)–(2), thereby finding the Pareto front for a baseline *connectivity* × *coverage* problem, mapping each objective value of each point in the Pareto front, thereby establishing the baseline performance parameters on the right-hand side of Eqs. (17)–(20). Then, we evaluate how the Pareto front changes relative to the baseline when the budget corresponding to connections removed from the baseline is instead allocated to specific objectives. This provides further insight into the trade-offs and yields distinct sets of non-dominated solutions to the decision-maker.

4. Solution method

To solve the proposed multi-objective formulation in Section 3, we utilise a two-phase process. Firstly, considering that the cycle network needs to be connected to be conducive to active transportation and fit for purpose (Natera Orozco et al., 2020) and that any planning will need to adhere to budget constraints, we build a *connectivity* × *coverage* set of non-dominated solutions (or Pareto front). This is detailed in

Table 2
Notations.

Sets	
G	Network graph
N	Nodes
E	Edges
P	Zoned nodes
Z	Zones
Attributes	
c_{ij}	Cost to link nodes i and j via a cycle-way
q_{ij}	Quietness contribution of link (i,j)
e_{ij}	Equity contribution of link (i,j)
Parameters	
α	Coverage (1) bound
β	Total cost (2) bound
δ	Quietness (3) bound
γ	Equity (4) bound
Θ	Maximum reduced coverage target
Binary variables	
x_{ij}	Whether edge (i,j) is selected for cycling expansion
y_{ab}	Whether zone a is connected to zone b
f_a	Whether zone a reaches at least one other zone
b_a	Whether zone a is reached by at least one other zone
ϕ_{ija}	Whether edge (i,j) is on a path that starts on zone a

Section 4.1, and the set of solutions is a baseline scenario for the other objectives to improve upon.

In the second phase, detailed in Section 4.2, we introduce flexibility to accommodate the other objectives, i.e., quietness and equity. This is done by removing a prescribed number of connections from each solution in the baseline cost-and-connectivity Pareto front whilst maintaining the same budget originally obtained for the baseline solution. With this fixed budget and reduced coverage requirements, we optimise different combinations of quietness and equity. The rationale is to generate new solutions that improve upon the latter objectives relative to the baseline Pareto front, as the additional budget afforded by the reduced coverage requirement will be utilised to improve the remaining objectives, as described below.

4.1. Cost-and-connectivity Pareto front

To construct the cost-and-coverage Pareto front, we will use the fact that the summation of $b_a(f_a)$ in Eq. (1) is bounded to $|Z|-1$, as each zone in set Z can reach (be reached by) at most the remaining $|Z|-1$ zones; here the operator $|\cdot|$ denotes the cardinality of a set. Hence, to build the Pareto front, one needs only consider a single-objective problem that minimises the budget requirement for each possible level of network connectivity, ranging from 0 to $Z-1$ connections. For each connectivity level, this is equivalent to solving the single-objective problem $P2$ in Definition 1 of Appendix.

The procedure is detailed in Algorithm 1. Note that Step 3 finds the minimal cost solution for each possible connectivity level by solving the auxiliary single objective Problem $P2$ in Definition 1 of Appendix. The solution $s=(E_s,W_s)$ obtained in this step comprises a set of selected edges $E_s=\{(i,j)|x_{ij}=1\ \forall(i,j)\in E\}$ and a set of directly connected origin–destination pairs $W_s=\{(a,b)|y_{ab}=1\ a,b\in Z, a\neq b\}$ associated to the minimum cost network expansion to attain the corresponding level of network connectivity. These will suffice to evaluate the solution's performance for each objective in the formulation ((1)–(4)).

Algorithm 1 outputs the set of solutions belonging to the cost-and-coverage Pareto front. These solutions will be provided to the decision maker to allow an informed decision based on the cost-coverage trade-offs. Hence, these solutions configure a baseline scenario that we call $A0$ onward. To enrich the menu of solutions to be considered further, we will add design flexibility to tackle the remaining objectives: quietness and equity. For each solution in set R, this flexibility will be

Algorithm 1: Cost and Coverage Pareto front

Data: Graph G
Result: Set of multi-objective solutions R.
1 $R \leftarrow \emptyset$;
2 **for** $\alpha_1 \in \{1,2,...|Z|-1\}$ **do**
3 $\quad s_{A0} \leftarrow$ solution of $P2(2*\alpha_1,\infty,0,0)$ from Definition 1 ;
4 $\quad R \leftarrow R \cup s_{A0}$;
5 **return** R

provided by allowing the removal of up to $\Theta > 0$ network connections whilst keeping the same budget; this will allow us to redirect the budget corresponding to the removed connections to provide improved solutions in terms of quietness and equity, as detailed next.

4.2. Additional Pareto sets with quietness and equity optimisation

To include improved solutions in terms of quietness and equity to the decision-maker's menu, we remove some connections from each baseline solution in R and reallocate the corresponding budget in four different scenarios:

1. $A1$ - Quietness focused- utilising the corresponding budget to maximise quietness;
2. $A2$ - Equity focused - utilising the corresponding budget to maximise equity;
3. $A3$ - Balanced quietness first - utilising the first half of the corresponding budget to maximise quietness, then fixing this as the new quietness requirement for a second step, where the remaining budget is allocated to further optimise equity;
4. $A4$ - Balanced equity first - utilising the first half of the corresponding budget to maximise equity and setting this as a requirement for a second step, where the remaining budget is allocated to further optimise quietness.

The first two scenarios, $A1$ and $A2$, explore the compromise between decreased connectivity and a single remaining objective, either quietness or equity. They provide the decision-maker with insights into the trade-offs between connectivity and quietness, or between connectivity and equity, under a fixed budget, whilst including additional network design options in their solution menu.

The third and fourth scenarios, $A3$ and $A4$, are inspired by the principles of goal programming, evaluating what happens when we use half the budget for either quietness or equity to establish a new baseline and then allocate the other half to the remaining objective, whilst keeping the new baseline for the objective that was considered first. This allows us to evaluate whether the order of budget allocation between quietness and equity affects the quality and configuration of the resulting solution, providing additional decision-making insights and further enriching the decision-maker's solution menu. Next, we detail the procedure for deriving the four additional solutions enumerated earlier for each baseline solution in the cost-and-coverage Pareto front, as outlined in Algorithm 2 below.

To facilitate the readability of Algorithm 2, we represent the four objectives of any feasible solution s to the multi-objective problem (Eqs. (1)–(4)) respectively as $\alpha(s)$, $\beta(s)$, $\delta(s)$, and $\gamma(s)$. Note that the Algorithm utilises the auxiliary single-objective problems in Definitions 2 and 3 from Appendix.

Step 2 of Algorithm 2 considers perturbations to each solution in the cost-and-coverage Pareto front described in Section 4.1. The perturbations allow the algorithm to remove $1\leq\theta\leq\Theta$ connections from each solution in the cost-and-coverage set (Step 4). Step 5 finds the corresponding solution in the cost-and-coverage Pareto front with θ fewer connections, as this allows us to quantify the additional budget required for the last θ connections.

Algorithm 2: Multi-objective solver

Data: Graph G, maximum past coverage target Θ, baseline cost-and-coverage Pareto front $\bar{R}$

Result: Final of multi-objective solutions R.

1 $R \leftarrow \bar{R}$;
2 **for** *each solution* $s \in \bar{R}$ **do**
3   **for** $\theta \in \{1, 2, \ldots \Theta\}$ **do**
4     $\alpha_2 \leftarrow \alpha(s) - \theta$;
5     $s'' = \{s* \in \bar{R} : \alpha(s*) = \alpha(\theta)\}$
6   **if** $\alpha(\theta) \geq 0$ **then**
7       $s_{A1} \leftarrow$ solution of $P3(2 * \alpha_2, \beta(s), 0, 0)$
8       $s_{A2} \leftarrow$ solution of $P4(2 * \alpha_2, \beta(s), 0, 0)$
9       $s' \leftarrow$ solution of $P3\left(2 * \alpha_2, \frac{\beta(s) + \beta(s'')}{2}, 0, 0\right)$
10       $s_{A3} \leftarrow$ solution of $P4\left(2 * \alpha_2, \beta(s), \delta(s'), 0\right)$
11       $s' \leftarrow$ solution of $P4\left(2 * \alpha_2, \frac{\beta(s) + \beta(s'')}{2}, 0, 0\right)$
12       $s_{A4} \leftarrow$ solution of $P3\left(2 * \alpha_2, \beta(s), 0, \gamma(s')\right)$
13       $R \leftarrow R \cup \{s_{A1}, s_{A2}, s_{A3}, s_{A4}\}$;
14 **return** R

Within the loop, Step 7 finds a solution, for scenario $A1$, that utilises the budget of the last θ connections to optimise further quietness — Objective (3). Correspondingly, Step 8 finds another solution, for scenario $A2$, that utilises the budget of the last θ connections to optimise further equity — Objective (4). We then use Step 9 to find a solution that uses the first half of the budget of the last θ connections to optimise quietness. The quietness performance of this intermediate solution is then passed as a requirement to Step 10, where we use the remaining budget to further optimise for equity. This generates a solution for scenario $A3$, a compromise between quietness and equity, starting with quietness.

To generate another compromise solution, Step 12 allocates the last half of the budget for the last θ connections to optimise equity under a quietness requirement established in Step 11, where the first half of the budget is dedicated to improving quietness, generating a solution for scenario $A4$. Finally, Step 13 adds the four newly obtained solutions to the final solution set to be presented to the decision maker.

To provide a clear visual overview of the solution methodology, Fig. 2 presents a flowchart of the proposed two-phase approach. The process initiates with Phase 1, detailed in Section 4.1, which generates the baseline Pareto front by optimising connectivity against cost (Objectives (1) × (2)). These non-dominated solutions serve as the input for Phase 2, where the surplus budget is iteratively reallocated to enhance quietness and equity, as detailed in Section 4.2.

The next section features experimental results utilising open-source cycle network data from the city of Southampton, England. These will illustrate the proposed approach's decision-support capabilities and trade-offs between the objectives.

5. Experimental results

Real-world data from Southampton's cycle network, sourced from OpenStreetMaps (OpenStreetMap contributors, 2017) and other auxiliary sources, were gathered using Python scripts, exported as an instance, and the algorithms and model were coded in C and compiled with GCC. The MIP solver used is Gurobi 11.01 (Gurobi Optimization, LLC, 2023), with a time limit of 3600 s per model. If the time limit is reached, the best solution so far and optimality gap are retrieved. The computer used in all experiments was an AMD Ryzen 7950x 16c/32t processor, 96 GB DDR5 of RAM, running Ubuntu 24.04 x64. The following sections detail our data sources, parameters, experimental setup, results, and analysis.

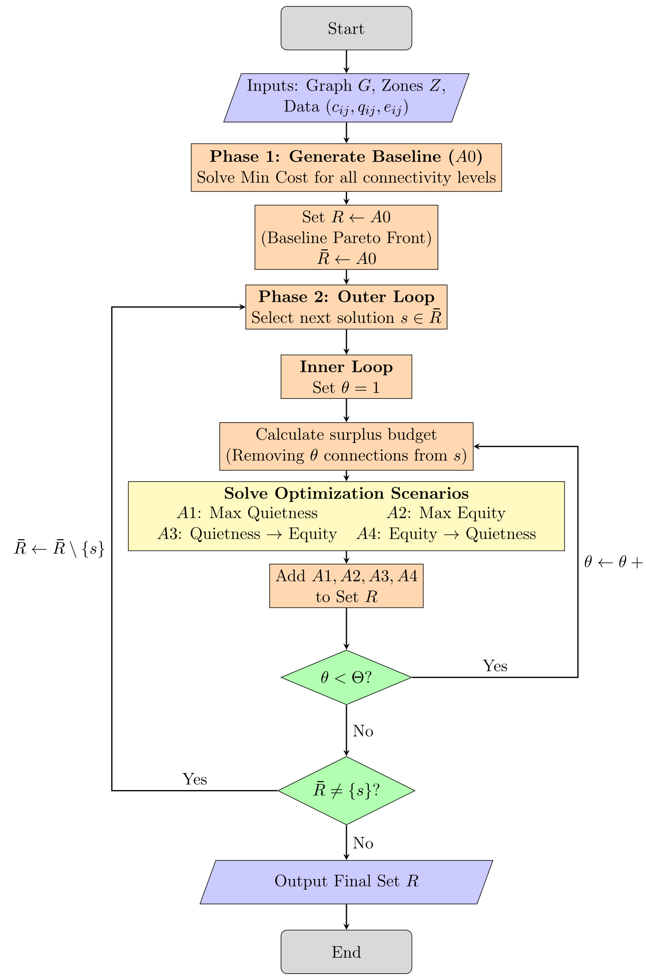

Fig. 2. Flowchart of the solution process.

5.1. Data sources and problem attributes

This section will provide details on the process for extracting data from the data sources, including the utilised application programming interfaces (APIs) and filter properties. Except for the green spaces polygons, all of our data sources are openly available. While it is possible to retrieve Green space polygons from *OpenStreetMaps* (OpenStreetMap contributors, 2017), a consultation with Southampton City Council revealed that other data sources were more accurate. Specifically, our formulation used data obtained for five separate layers of the open map data, as described below:

- **Road network**: We utilised the `osmnx` API[1] to query OpenStreetMap (OSM) data. Specifically, we used the `graph_from_place` function with the filter `network_type='all'` to retrieve the complete drivable and walkable topology for the Southampton area. The raw data was parsed into a NetworkX MultiDiGraph. For each edge, the attributes `length` and `maxspeed` were extracted. For `maxspeed`, where missing, a default baseline of 5 mph was imputed to penalise undefined routes in the quietness objective.
- **Existing cycling network**: To map the current infrastructure, we performed a secondary query using the `osmnx` filter `network_type='bike'` and the custom filter `['cycleway']` to

[1] https://osmnx.readthedocs.io/en/stable/.

identify edges with dedicated cycling infrastructure. These edges were flagged within the master road network graph to define the initial set of "Cycle Zones".

- **Green spaces polygons**: High-fidelity green space data was obtained from the "Ordnance Survey (OS) MasterMap Greenspace Layer"[2] as vector polygons (GML format). The data was filtered to retain only functional leisure spaces with the attributes "Natural", "Play Space", "Playing Field", or "Public Park". To integrate this with the network graph, we performed a spatial join operation. Any edge (i,j) in the road network was classified as "inside" a green zone if both its start node i and end node j were geographically located within a Green Space polygon.
- **IMD zones**: Socio-economic data was sourced from the UK's ministry of housing, communities, and local government as a shapefile containing lower layer super output areas (LSOAs) and their associated 2019 indices of multiple deprivation (IMD).[3] Parsing involved a point-in-polygon operation to assign an IMD score to every node in the network graph based on its coordinates. This spatial mapping enables dynamic calculation of the equity contribution of any potential route based on the neighbourhood deprivation levels traversed.

Given our data sources, the calculated values of c_{ij}, q_{ij} and e_{ij} are the following:

- **Construction cost** c_{ij}: Since we do not locate different types of cycle-ways and our road network source is not very detailed, we assume that the construction cost is proportional to the road's length. Hence, for the sake of simplicity, we assume that c_{ij} is equal to the length of the road segment $(i,j) \in E$; therefore, it will be measured in metres in our experiments.
- **Quietness contribution** q_{ij}: As a proxy for safety, we assume that the quietness of an edge is inversely proportional to its speed limit. Hence, in our experiments, we set q_{ij} as the length of edge $(i,j) \in E$ divided by its speed limit.
- **Equity contribution** e_{ij}: Given the layer with the IMD zones, each node was mapped to a corresponding IMD score. The IMD score of a zone is a positive number, in which the larger numbers indicate a less deprived zone. Knowing that smaller IMD values indicate a more deprived area, the equity contribution of an edge e_{ij} is set as the length of edge $(i,j) \in E$ divided by the average IMD score for nodes i and j.

To illustrate these parameter definitions numerically using the network example in Fig. 1, consider a candidate edge (i,j) representing a potential cycle lane connecting Zone C to Zone F with a length of 300 m. If this segment is located on a quiet residential street with a speed limit of 20 mph and passes through a deprived area with an average IMD score of 10, the parameters would be calculated as follows: the cost $c_{ij} = 300$; the quietness contribution $q_{ij} = 300/20 = 15$; and the equity contribution $e_{ij} = 300/10 = 30$. Conversely, if an alternative route of the same length (300 m) existed on a faster road (30 mph) in a less deprived area (IMD score 50), the values would be $c_{ij} = 300$, $q_{ij} = 300/30 = 10$, and $e_{ij} = 300/50 = 6$. In view of objectives (3) and (4), the model would prioritise the first segment, as it offers higher contributions to both quietness ($15 > 10$) and equity ($30 > 6$) for the same construction cost.

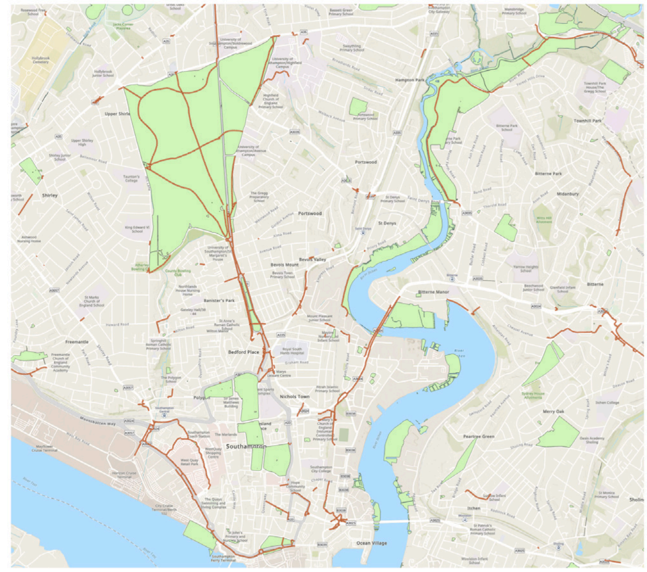

Fig. 3. Selected test instance. *Source:* ArcGIS Pro with the existing cycling network (brown) and green spaces (green) layers.

5.2. Experimental setup

Fig. 3 overviews our selected test instance, which includes a large part of the city of Southampton. Located on the South coast of England, this area features a good distribution of green and blue zones and a diverse set of IMD indices. The zones highlighted in green are the *green zones*. Often referred to as *green spaces*, these zones are usually intended for leisure. Conversely, the highlighted road segments in brown represent the existing cycling infrastructure, which is split into connected *cycle zones* in our modelling approach. When specific green and cycle zones are fully interconnected, they are treated as a single connected zone in the model. For instance, the two green zones at the bottom of Fig. 3 and the cycle infrastructure that connects them are treated as a single connected zone in the model. The overall network contains 77,745 edges, 37,653 nodes, and 128 disconnected zones. Given this, and knowing that Algorithm 1 solves the model once per $|Z| - 1$ (Line 3) and Algorithm 2 solves it $6 \times \Theta$ more times (Lines 7–12), our multi-objective algorithm solved the problem 3175 times. Among these executions, 131 cases were not optimal, with the largest optimality gap of 4.43%. The whole execution took around 520 h.

5.3. Results and analysis

As detailed in Section 4, our multi-objective algorithm evaluates five possible scenarios for spending the same amount. The baseline $A0$ is the cost-and-coverage Pareto front. As detailed in Section 4.1, each solution features the minimum cost solution β to attain a certain number of connections.

Scenarios $A1$ to $A4$ utilise the same budget as $A0$ but reduce the number of connections to allow extra-budgetary flexibility to improve the remaining objectives, as detailed in Section 4.2. Scenario $A1$ further optimises quietness only, and Scenario $A2$ further optimises for equity only. Scenarios $A3$ and $A4$ are compromise scenarios that utilise half the budget for quietness and the other half for equity, but in different orders. Scenario $A3$ first establishes the quietness threshold, while Scenario $A4$ maximises equity first. The remainder of this section displays and discusses the results: firstly, the baseline scenario $A0$ in Section 5.3.1 and then the alternative spending scenarios $A1 - A4$ in

[2] https://www.ordnancesurvey.co.uk/products/os-mastermap-greenspace-layer.

[3] https://data-communities.opendata.arcgis.com/datasets/5e1c399d787e48c0902e5fe4fc1ccfe3/about.

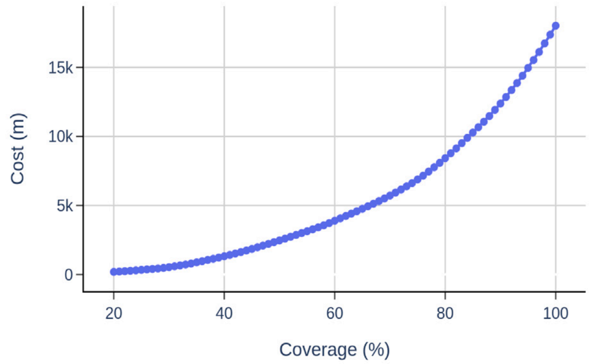

Fig. 4. Optimal Pareto between maximising relative coverage (%) (1), on the horizontal axis, and minimising cost (2) in metres of new cycle lanes.

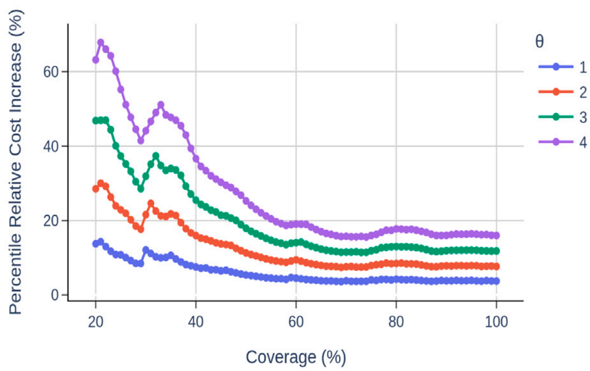

Fig. 5. Relative cost increase for each added θ connections.

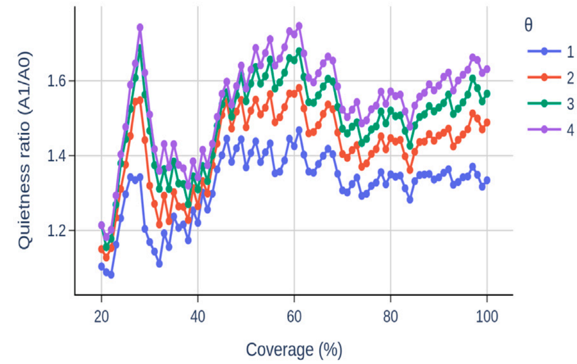

Fig. 6. Relative quietness ratio for Scenario A1 with respect to Scenario A0, with θ less connections and fixed budget.

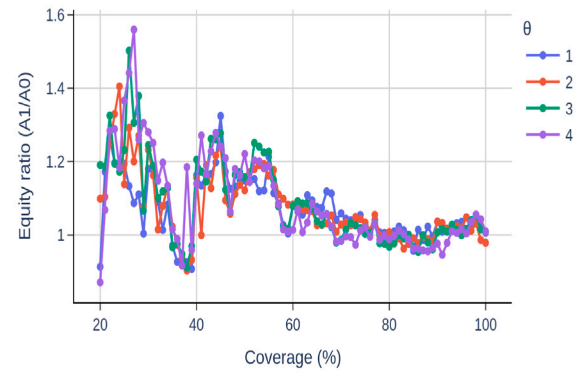

Fig. 7. Relative equity ratio of Scenario A1 with respect to Scenario A0, with θ less connections and fixed budget.

Section 5.3.2. Finally, Section 5.3.3 features a graphical visualisation of solutions highlighting the suggested infrastructure with different priorities.

5.3.1. Baseline scenario (A0)

Fig. 4 conveys the cost-and-coverage Pareto front — Scenario $A0$, where the incremental cost for each additional connection seems to be exponential. To help us analyse the remaining scenarios and to provide further insights to the decision maker, Fig. 5 conveys the additional percentage increase in cost if one adds $1 \leq \theta \leq \Theta$ connections to each baseline solution, where $\Theta = 4$, and shows that the variation in cost fluctuates when the network's connection level is low, stabilising for higher levels of coverage. The fluctuation is expected, given that we will need to reach unserved areas to improve coverage, which may eventually be outside the current network boundaries. However, as the network expands, the variation stabilises. Indeed, it is clear in our example that the percentage increase in cost for extra connections stabilises when we reach around 60% of coverage. Specifically, for any coverage target over 60%, the incremental cost for each connection is around 3.8%. The alternative scenarios in the remainder of this section will analyse, for each coverage level, how much the other objectives can be improved with the equivalent amount that would be saved with θ fewer connections.

5.3.2. Alternative scenarios (A1-A4)

Our alternative spending analysis starts with Figs. 6 and 7 of Scenario $A1$'s results. This scenario allows the model to eliminate θ connections from the baseline cost-and-coverage Pareto front whilst optimising solely for quietness. Fig. 6 depicts the relative ratio of quietness between each point in $A1$ with the same budget as $A0$, for each value of θ. As expected, we observe an increase in quietness at each coverage level; furthermore, we find that larger increases are possible by removing more connections. Also, observe that the increases tend to fluctuate more for low coverage values and become more stable as coverage surpasses 45%. Analogously, Fig. 7 conveys the ratio of equity between each point in $A1$ at the same budget as in $A0$, which also shows an oscillating behaviour for lower coverage and stability for coverage levels over 60%, independent of the value of θ. The equity ratio relative to the baseline stabilises around 1, indicating that equity values are generally indistinguishable from those in the baseline scenario. This is expected, given that $A1$ does not optimise for equity.

Fig. 9 depicts the average ratio of the equity measure with respect to the baseline for distinct coverage levels. The results are similar to those observed for quietness maximisation in $A1$. We observe considerable gains in equity, which fluctuate at low coverage levels and stabilise at coverage levels above 60%. It is also apparent that the gains increase with the number of removed connections, θ, as expected. Finally, as Scenario $A2$ optimises for equity, one can see in Fig. 8 that the quietness levels are independent of θ and indistinguishable from those in the baseline scenario. Once again, the ratio relative to the baseline fluctuates more significantly at lower coverage levels and stabilises around one.

We now analyse $A3$, which considers a compromise between quietness and equity by first optimising for quietness with an intermediary budget to establish a minimum quietness requirement and then optimising for equity. Figs. 10 and 11 convey the relative gains with respect to the baseline for each objective. In contrast with $A1$ and $A2$, we now observe considerable gains in both objectives. As expected, the gains grow with the number of removed connections θ. Observe also that the trend observed in Fig. 11 is identical to that in the single-side approach in Scenario $A2$, see Fig. 9, where only equity was maximised.

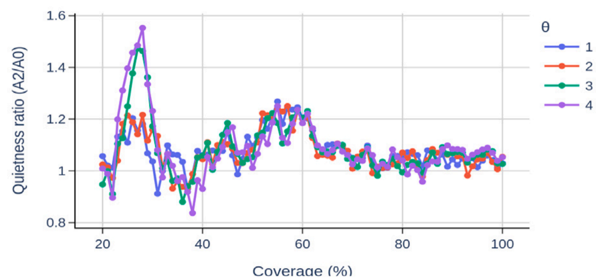

Fig. 8. Relative quietness ratio for Scenario A2 with respect to Scenario A0, with θ less connections and fixed budget.

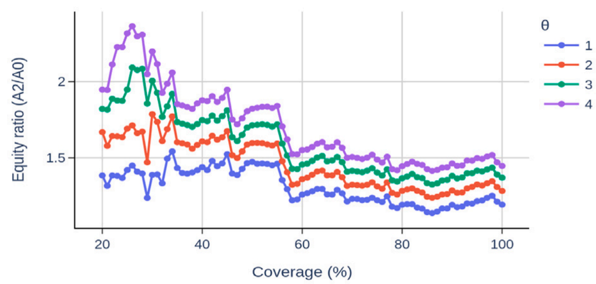

Fig. 9. Relative equity ratio of Scenario A2 with respect to Scenario A0, with θ less connections and fixed budget.

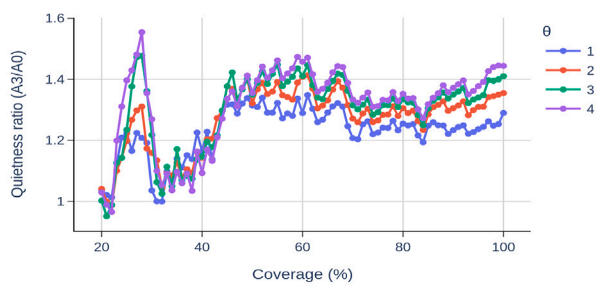

Fig. 10. Relative quietness ratio of Scenario A3 with respect to Scenario A0, with θ less connections and fixed budget.

Finally, Figs. 12 and 13 first maximise equity and then quietness. Similarly to $A3$, we also observe significant gains for all coverage levels, and the gains increase with the number of removed connections θ. They also tend to stabilise once coverage surpasses 60%. Similarly to $A3$, the objective optimised last, which in $A4$ is quietness, exhibits the same trend as the single-sided approach ($A1$). This is apparent when we compare Figs. 6 to 12.

The previous results provide some interesting insights. As expected, if we are interested in only one additional objective, either quietness or equity, then considering the scenario that optimises for this objective is the appropriate choice. Indeed, a simple inspection of the results shows that $A1$ exhibits better quietness performance than $A2$–$A4$. Similarly, $A2$ performs better concerning equity than $A1$, $A3$, and $A4$. However, in $A1$ and $A2$, the neglected objectives perform very similarly to the baseline scenario $A0$.

Furthermore, the results show that a more balanced approach to allocating the budget between quietness and equity yields significant gains for both objectives, which are not achievable in single-sided scenarios. Moreover, since the balanced scenarios exhibit a very similar trend to the single-sided ones for the objectives optimised last, we can conclude that the application of $A3$ is preferred when the decision-maker prioritises equity, and $A4$ when the decision-maker prioritises quietness.

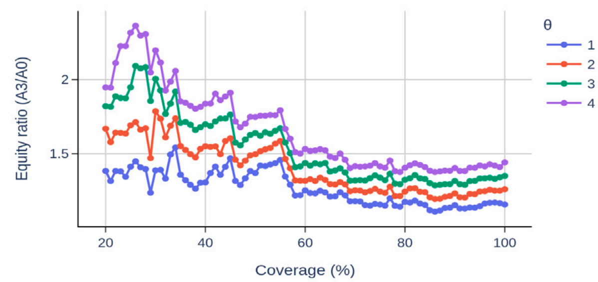

Fig. 11. Relative equity ratio of Scenario A3 with respect to Scenario A0, with θ less connections and fixed budget.

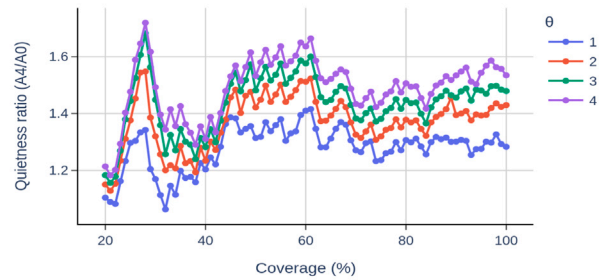

Fig. 12. Relative quietness ratio for Scenario A4 with respect to Scenario A0, with θ less connections and fixed budget.

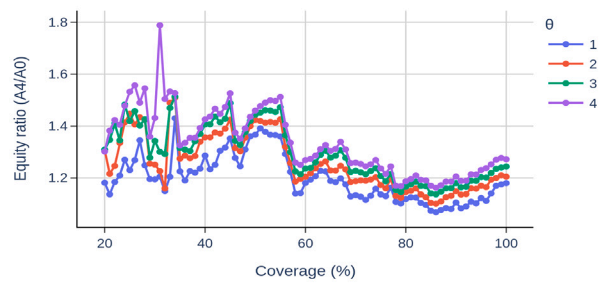

Fig. 13. Relative equity ratio for Scenario A4 with respect Scenario A0, with θ less connections and fixed budget.

In the next section, we will explore the geographical composition of the solution in Southampton's map. For brevity, we will discuss one solution in the baseline scenario $A0$ and then describe the adjustments to this solution as we consider the scenarios in Section 5.3.2.

5.3.3. *Visualisation of the solutions*

Fig. 14 uses the same colour representation for the green spaces (green) and the existing cycling infrastructure (brown) and presents the visualisation of a solution (yellow) from the *cost and coverage* Pareto set $A0$ depicted in Section 5.3.1, with 90% coverage. Note that, as expected, the suggested infrastructure in yellow primarily connects the zones via the shortest possible paths.

An important feature of the solution in Fig. 14 is that it generates fully connected paths between existing cycle infrastructures and green and blue areas. This highlights the effectiveness of the approach to enforce connected, functional cycle infrastructure and access to green and blue spaces. By preventing cycle network designs comprising disconnected patches, which are often present in current infrastructure, discouraging users (Natera Orozco et al., 2020), and introducing safety issues (Barrero and Rodriguez-Valencia, 2022), our approach provides a tool to support the essential leap towards cyclist-centred planning.

Fig. 14. Solution example with 90% coverage on the baseline scenario A0 (yellow).
Source: ArcGIS Pro with the existing cycling network (brown) and green spaces areas (green) layers.

Fig. 15. Partial solution example when prioritising quietness on a Scenario A1 (blue) compared to the baseline scenario (yellow).
Source: ArcGIS Pro with the existing cycling network (brown) layer.

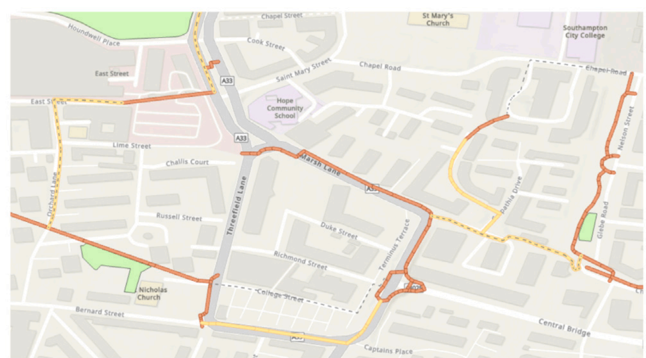

Fig. 16. Partial solution example when prioritising equity (dashed line) compared to the baseline scenario (yellow).
Source: ArcGIS Pro with the existing cycling network (brown) and green spaces (green) layers.

To illustrate the trade-offs with respect to quietness and equity under different network configurations, we will now analyse the differences between the baseline solution in $A0$ (Fig. 14) and the corresponding solutions in Scenarios $A1$ and $A2$, whilst removing $\theta = 1$ connection to focus the corresponding budget on improving either quietness or equity. Fig. 15 analyses the differences between the baseline solution and the one focusing on quietness (Scenario $A1$) for a specific area in the city map. The solution prioritising quietness (in blue) recommends quieter side lanes over the main lanes in the baseline. This is expected, highlights the flexibility in network design, and demonstrates that it is possible to focus on different aspects with similar budgets.

After spending the budget corresponding to the θ-removed connections to improve equity (Scenario A2), the resulting solution, shown in Fig. 16, coincides with the baseline solution in many segments, with slight adjustments to include more deprived areas in the design. This highlights the power of the approach to capture real-world trade-offs and recommend suitable adjustments whilst maintaining a comparable budget.

5.4. Discussion

The proposed model demonstrates high transferability across other geographic settings because it relies on standard spatial datasets, including road and cycling networks, green and blue space distributions, and regional deprivation indices. Given OpenStreetMap's extensive global coverage and its reliable inclusion of green-space data, this methodology applies to any urban environment where such open-source data are available. Furthermore, implementation by local governing bodies would likely provide access to higher-resolution proprietary road and city models.

Also, to facilitate immediate adoption in real-world scenarios, the proposed method is designed as a modular decision-support tool that can integrate with existing local authority planning frameworks. For practical applications, the model's cost structure can be readily adapted to reflect specific infrastructure types (e.g., distinguishing between painted lanes and fully segregated paths) and to account for context-specific constraints (e.g., land acquisition). Furthermore, this framework provides a robust foundation for future studies to address the temporal nature of urban development. Subsequent research should aim to extend this approach into a dynamic modelling environment, optimising the sequencing of network improvements to align with long-term strategic goals and fractional budget allocations.

By addressing these limitations, the tool can evolve into an even more powerful resource for urban planners and policymakers. The core strength of our approach — making the compromises between cost, coverage, safety, and equity explicit — provides a solid foundation for future development. Ultimately, this work supports the ongoing effort to develop sustainable, safe, and equitable cycling infrastructure that is truly user-centred.

6. Concluding remarks

This work introduces a novel formulation for designing cycle networks that focuses on creating connected, cycle-friendly networks that access green and blue spaces. This aligns with the worldwide trend towards sustainable transportation and an improved quality of life through access to green and blue spaces, while also contributing to reduced healthcare burden and improved environmental indicators, such as air pollution. We applied the model to the city of Southampton. The results illustrate the approach's power in equipping the decision-maker with a menu of solutions that strike different compromises among cost, coverage, quietness, and equity. They also explore specific aspects of compromises between a baseline focused solely on cost and coverage and more balanced solutions that consider quietness and equity, either individually or in various combinations. The results show that a balanced approach, which simultaneously considers multiple objectives, can yield significant improvements at the same cost as a single-objective approach focused solely on connectivity.

Among the avenues for future works, with suitable information about the area's topology, one can account for path inclination and penalise routes that traverse steep or hilly regions. One could also reward scenic routes or focus on routes within popular origin–destination pairs whenever reliable information on daily displacement patterns is available. Finally, the method's adaptability allows future work to refine the 'quietness' safety proxy by incorporating granular variables such as traffic volume, road width, and the presence of heavy goods vehicles, thereby more accurately reflecting user comfort.

CRediT authorship contribution statement

Bruno Salezze Vieira: Writing – original draft, Visualization, Validation, Software, Resources, Methodology, Formal analysis, Data curation. **Ranga Abeysooriya:** Writing – review & editing, Visualization, Validation, Methodology, Data curation. **Dawn-Marie Walker:** Writing – review & editing, Supervision, Project administration, Investigation, Funding acquisition, Formal analysis, Conceptualization. **Edilson F. Arruda:** Writing – original draft, Validation, Supervision, Methodology, Investigation, Formal analysis.

Declaration of competing interest

The authors declare the following financial interests/personal relationships which may be considered as potential competing interests: Bruno Salezze Vieira reports financial support was provided by Engineering and Physical Sciences Research Council. If there are other authors, they declare that they have no known competing financial interests or personal relationships that could have appeared to influence the work reported in this paper.

Acknowledgements

We would like to thank the Southampton City Council's specialists in sustainability and transport for engaging with the project and providing feedback and support. We are grateful to Rebecca Collins for her support on map data sources and the definition of the equity measure. This work was supported by the Engineering and Physical Sciences Research Council, United Kingdom (EPSRC) "Infrastructure for Port Cities and Coastal Towns (iPACT)" network under the project "Coastal Connections: Systems and Synergy".

Appendix. Auxiliary single objective formulations

This appendix explores the auxiliary single-objective formulations used to compose the Pareto front of the multi-objective formulation introduced in Section 3. We will define three specific problems for the second, third and fourth objectives: Eqs. (2)–(4). This is because we will enumerate all possible coverage solutions, i.e., all possible values of the first objective in Eq. (2); hence, we will not need to define a specific optimisation for this objective. Each auxiliary problem is defined separately in the remainder of this appendix.

Definition 1. Problem $P_2(\alpha, \beta, \delta, \gamma)$

$$\text{Maximise} \quad z_2 = \sum_{(i,j)\in E} c_{ij} x_{ij}, \quad \text{subject to: (5)–(20),} \tag{A.1}$$

where α, β, δ, and γ are the right hand side parameters in Eqs. (17)–(20).

Definition 2. Problem $P_3(\alpha, \beta, \delta, \gamma)$

Let x^* be the solution of the following optimisation problem:

$$\text{Maximise} \quad z_3 = \sum_{(i,j)\in E} q_{ij} x_{ij}, \quad \text{subject to: (5)–(20),} \tag{A.2}$$

where α, β, δ, and γ are the right hand side parameters in Eqs. (17)–(20).

Definition 3. Problem $P_4(\alpha, \beta, \delta, \gamma)$

Let x^* be the solution of the following optimisation problem:

$$\text{Maximise} \quad z_4 = \sum_{(i,j)\in E} e_{ij} x_{ij}, \quad \text{subject to: (5)–(20),} \tag{A.3}$$

where α, β, δ, and γ are the right hand side parameters in Eqs. (17)–(20).

To tackle each individual single-objective problem from Definitions 1 to 3, we utilise a standard Branch and Cut algorithm described in the next subsection.

A.1. Branch-and-cut (B&C)

Branch-and-cut was conceived for problems with a large number of constraints, whereby a proposed solution to the problem is fed into a separation problem, which verifies whether the solution is feasible; if not, the separation problem returns a set of violated constraints (Dantzig and Wolfe, 1960). In the formulation of Section 3, specifically, there are a large number of sub-tour constraints (12). Hence, we use the branch-and-cut framework for this set of constraints by eliminating them from the formulation and then gradually adding the violated constraints of each new solution found in the iterative procedure, as the branch-and-cut procedure prescribes.

More specifically, for each solution s, we build a connected zones network $G_s^y = (Z, W_s)$ that considers each zone as a node, and each pair of zones $(a, b) \in W_s$ as an edge between zones, from a to b. Any cycle on G_y implicates a violated constraint in Eq. (12). This way, for each connected zone network G_y, a Depth First Search (DFS) (Bondy and Murty, 1976) algorithm is executed starting in each zone; if a cycle is found for a given solution s, we know that the zones in the cycle comprise a set of constraints in Eq. (12), which is then added to the model. We then discard the infeasible solution s and continue the algorithm. Otherwise, s is a valid solution, and no new constraint needs to be added.

References

Aldred, R., Watson, T., Lovelace, R., Woodcock, J., 2019. Barriers to investing in cycling: Stakeholder views from England. Transp. Res. A: Policy Pract. 128, 149–159. http://dx.doi.org/10.1016/j.tra.2017.11.003.

Aultman-Hall, L., Hall, F.L., Baetz, B.B., 1997. Analysis of bicycle commuter routes using geographic information systems: Implications for bicycle planning. Transp. Res. Rec. 1578 (1), 102–110. http://dx.doi.org/10.3141/1578-13, arXiv:https://doi.org/10.3141/1578-13.

Barrero, G.A., Rodriguez-Valencia, A., 2022. Asking the user: a perceptional approach for bicycle infrastructure design. Int. J. Sustain. Transp. 16 (3), 246–257. http://dx.doi.org/10.1080/15568318.2020.1871127, arXiv:https://doi.org/10.1080/15568318.2020.1871127.

Bondy, J.A., Murty, U.S.R., 1976. Graph Theory with Applications. vol. 290, Macmillan, London.

Caicedo, A., Estrada, M., Medina-Tapia, M., Mayorga, M., 2023. Optimizing bike network design: A cost-effective methodology for heterogeneous travel demands using continuous approximation techniques. Transp. Res. A: Policy Pract. 176, 103826. http://dx.doi.org/10.1016/j.tra.2023.103826, URL https://www.sciencedirect.com/science/article/pii/S096585642300246X.

Cunha, I., Silva, C., 2023. Equity impacts of cycling: examining the spatial-social distribution of bicycle-related benefits. Int. J. Sustain. Transp. 17 (6), 573–591. http://dx.doi.org/10.1080/15568318.2022.2082343, arXiv:https://doi.org/10.1080/15568318.2022.2082343.

Dales, J., Jones, P., Black, R., Hoe, N., Loy, P., Mayo, A., Parkin, J., Strong, M., 2014. International Cycling Infrastructure Best Practice Study. Technical Report, Transport for London, Prepared by Urban Movement and Phil Jones Associates.

Dantzig, G.B., Wolfe, P., 1960. Decomposition principle for linear programs. Oper. Res. 8 (1), 101–111. http://dx.doi.org/10.1287/opre.8.1.101.

Davis, A., 2010. Value for Money: An Economic Assessment of Investment in Walking and Cycling, Research Report, fifth ed. Bristol City Council and NHS Bristol.

de Oliveira, S.P., Luche, J.R.D., Marins, F.A.S., da Silva, A.F., Costa, A.F.B., 2021. Design of a Bike–Bus network for a city of half a million citizens. J. Urban Plan. Dev. 147 (3), 04021029. http://dx.doi.org/10.1061/(ASCE)UP.1943-5444.0000709, arXiv:https://doi.org/10.1061/(ASCE)UP.1943-5444.0000709.

Deb, K., Deb, K., 2014. Multi-objective Optimization. In: Search Methodologies: Introductory Tutorials in Optimization and Decision Support Techniques. Springer US, Boston, MA, pp. 403–449. http://dx.doi.org/10.1007/978-1-4614-6940-7_15.

Duthie, J., Unnikrishnan, A., 2014. Optimization framework for bicycle network design. J. Transp. Eng. 140 (7), 04014028. http://dx.doi.org/10.1061/(ASCE)TE.1943-5436.0000690, arXiv:https://doi.org/10.1061/(ASCE)TE.1943-5436.0000690.

Gössling, S., Kees, J., Hologa, R., Riach, N., von Stülpnagel, R., 2024. Children's safe routes to school: Real and perceived risks, and evidence of an incapacity-incapability space. J. Cycl. Micromobility Res. 2, 100019. http://dx.doi.org/10.1016/j.jcmr.2024.100019, URL https://www.sciencedirect.com/science/article/pii/S295010592400010X.

Guler, D., Yomralioglu, T., 2021. Bicycle station and lane location selection using open source GIS technology. In: Open Source Geospatial Science for Urban Studies: The Value of Open Geospatial Data. Springer International Publishing, Cham, pp. 9–36. http://dx.doi.org/10.1007/978-3-030-58232-6_2.

Gurobi Optimization, LLC, 2023. Gurobi Optimizer Reference Manual. URL https://www.gurobi.com.

Kilani, M., Bennaya, S., 2023. Environmental impacts of bicycling in urban areas: A micro-simulation approach. Transp. Res. D: Transp. Environ. 125, 103967. http://dx.doi.org/10.1016/j.trd.2023.103967, URL https://www.sciencedirect.com/science/article/pii/S1361920923003644.

Krenn, P.J., Oja, P., Titze, S., 2014. Route choices of transport bicyclists: a comparison of actually used and shortest routes. Int. J. Behav. Nutr. Phys. Act. 11 (1), 31. http://dx.doi.org/10.1186/1479-5868-11-31.

Krizek, K.J., Roland, R.W., 2005. What is at the end of the road? Understanding discontinuities of on-street bicycle lanes in urban settings. Transp. Res. D: Transp. Environ. 10 (1), 55–68. http://dx.doi.org/10.1016/j.trd.2004.09.005, URL https://www.sciencedirect.com/science/article/pii/S1361920904000628.

Le Gouais, A., Panter, J., Cope, A., Powell, J., Bird, E., Woodcock, J., Ogilvie, D., Foley, L., 2021. A natural experimental study of new walking and cycling infrastructure across the United Kingdom: The Connect2 programme. J. Transp. Health 20, 100968. http://dx.doi.org/10.1016/j.jth.2020.100968.

Liu, H., Szeto, W., Long, J., 2019. Bike network design problem with a path-size logit-based equilibrium constraint: Formulation, global optimization, and matheuristic. Transp. Res. E: Logist. Transp. Rev. 127, 284–307. http://dx.doi.org/10.1016/j.tre.2019.05.010, URL https://www.sciencedirect.com/science/article/pii/S1366554518307427.

Mauttone, A., Mercadante, G., Rabaza, M., Toledo, F., 2017. Bicycle network design: model and solution algorithm. Transp. Res. Procedia 27, 969–976. http://dx.doi.org/10.1016/j.trpro.2017.12.119, URL https://www.sciencedirect.com/science/article/pii/S2352146517310165, 20th EURO Working Group on Transportation Meeting, EWGT 2017, 4-6 September 2017, Budapest, Hungary.

Mitra, R., Khachatryan, A., Hess, P.M., 2021. Do new urban and suburban cycling facilities encourage more bicycling? Transp. Res. D: Transp. Environ. 97, 102915. http://dx.doi.org/10.1016/j.trd.2021.102915, URL https://www.sciencedirect.com/science/article/pii/S1361920921002145.

Natera Orozco, L.G., Battiston, F., Iñiguez, G., Szell, M., 2020. Data-driven strategies for optimal bicycle network growth. R. Soc. Open Sci. 7 (12), 201130. http://dx.doi.org/10.1098/rsos.201130, arXiv:https://royalsocietypublishing.org/doi/pdf/10.1098/rsos.201130 URL https://royalsocietypublishing.org/doi/abs/10.1098/rsos.201130.

Nath, R.B., Rambha, T., 2019. Modelling methods for planning and operation of Bike-Sharing systems. J. Indian Inst. Sci. 99 (4), 621–645. http://dx.doi.org/10.1007/s41745-019-00134-8.

OpenStreetMap contributors, 2017. Planet dump. retrieved from https://planet.osm.org. https://www.openstreetmap.org.

Ospina, J.P., Duque, J.C., Botero-Fernández, V., Montoya, A., 2022. The maximal covering bicycle network design problem. Transp. Res. A: Policy Pract. 159, 222–236. http://dx.doi.org/10.1016/j.tra.2022.02.004, URL https://www.sciencedirect.com/science/article/pii/S0965856422000325.

Paix, L.L., Cherchi, E., Geurs, K., 2021. Role of perception of bicycle infrastructure on the choice of the bicycle as a train feeder mode. Int. J. Sustain. Transp. 15 (6), 486–499. http://dx.doi.org/10.1080/15568318.2020.1765223, arXiv:https://doi.org/10.1080/15568318.2020.1765223.

Paulsen, M., Rich, J., 2023. Societally optimal expansion of bicycle networks. Transp. Res. B: Methodol. 174, 102778. http://dx.doi.org/10.1016/j.trb.2023.06.002, URL https://www.sciencedirect.com/science/article/pii/S0191261523000954.

Szell, M., Mimar, S., Perlman, T., Ghoshal, G., Sinatra, R., 2022. Growing urban bicycle networks. Sci. Rep. 12 (1), 6765. http://dx.doi.org/10.1038/s41598-022-10783-y.

Tiznado-Aitken, I., Mora, R., Oyarzun, G., Vergara, J., Vecchio, G., 2022. A bumpy ride: structural inequalities, quality standards, and institutional limitations affecting cycling infrastructure. Transp. Res. D: Transp. Environ. 110, 103434. http://dx.doi.org/10.1016/j.trd.2022.103434, URL https://www.sciencedirect.com/science/article/pii/S1361920922002607.

Winters, M., Teschke, K., Grant, M., Setton, E.M., Brauer, M., 2010. How far out of the way will we travel?: Built environment influences on route selection for bicycle and car travel. Transp. Res. Rec. 2190 (1), 1–10. http://dx.doi.org/10.3141/2190-01, arXiv:https://doi.org/10.3141/2190-01.

Zahabi, S.A.H., Chang, A., Miranda-Moreno, L.F., Patterson, Z., 2016. Exploring the link between the neighborhood typologies, bicycle infrastructure and commuting cycling over time and the potential impact on commuter GHG emissions. Transp. Res. D: Transp. Environ. 47, 89–103. http://dx.doi.org/10.1016/j.trd.2016.05.008, URL https://www.sciencedirect.com/science/article/pii/S136192091630270X.

Zhao, P., Li, S., 2017. Bicycle-metro integration in a growing city: The determinants of cycling as a transfer mode in metro station areas in Beijing. Transp. Res. A: Policy Pract. 99, 46–60. http://dx.doi.org/10.1016/j.tra.2017.03.003, URL https://www.sciencedirect.com/science/article/pii/S0965856416303925.

Zhu, S., Zhu, F., 2020. Multi-objective bike-way network design problem with space-time accessibility constraint. Transportation 47 (5), 2479–2503. http://dx.doi.org/10.1007/s11116-019-10025-7.

Zuo, T., Wei, H., 2019. Bikeway prioritization to increase bicycle network connectivity and bicycle-transit connection: A multi-criteria decision analysis approach. Transp. Res. A: Policy Pract. 129, 52–71. http://dx.doi.org/10.1016/j.tra.2019.08.003, URL https://www.sciencedirect.com/science/article/pii/S096585641831156X.